

Alkene ozonolysis SOA: inferences of composition and droplet growth kinetics from Köhler theory analysis

A. Asa-Awuku¹, A. Nenes^{1,2}, S. Gao^{3,*}, R. C. Flagan^{3,4}, and J. H. Seinfeld^{3,4}

¹School of Chemical and Biomolecular Engineering, Georgia Institute of Technology, Atlanta, GA, USA

²School of Earth and Atmospheric Sciences, Georgia Institute of Technology, Atlanta, GA, USA

³Department of Environmental Science and Engineering, California Institute of Technology, Pasadena, CA, USA

⁴Department of Chemical Engineering, California Institute of Technology, Pasadena, CA, USA

* now at: the Department of Atmospheric Science, University of Arizona, Tuscon, AZ, USA

Received: 7 June 2007 – Accepted: 14 June 2007 – Published: 26 June 2007

Correspondence to: A. Nenes (nenes@eas.gatech.edu)

Title Page

Abstract

Introduction

Conclusions

References

Tables

Figures

◀

▶

◀

▶

Back

Close

Full Screen / Esc

Printer-friendly Version

Interactive Discussion

EGU

Abstract

The CCN properties, surfactant characteristics, and droplet growth kinetics of secondary organic aerosol (SOA) formed from the ozonolysis of three parent alkene hydrocarbons (terpinolene, 1-methylcycloheptene and cycloheptene) are explored. Based on measurements of CCN activity, total carbon and inorganic ion concentrations, we estimate the average molar volume of the water-soluble organic component using Köhler Theory Analysis (KTA). The results suggest that the water-soluble organics in the SOA are composed of relatively low molecular weight species, with an effective molar mass less than 200 g mol^{-1} . This finding is consistent with the speciated fraction for some of the SOA, and suggests that KTA can be applied to complex organic aerosol, such as that found in the atmosphere. From measurements of CCN activity and Köhler Theory, we apply a novel method to infer the surface tension at the point of activation; this is used to infer the presence of surface-active organics. It is found that the water-soluble carbon can be surface-active, depressing surface tension 10–15% from that of pure water at concentrations relevant for CCN activation. Although important, this level of surface tension depression is lower than expected for HULIS, which suggest that they are not likely in the SOA examined. In all cases, the CCN exhibit droplet growth kinetics similar to $(\text{NH}_4)_2\text{SO}_4$.

1 Introduction

Aerosols, by acting as cloud condensation nuclei (CCN), have a profound impact on the hydrological cycle and climate. Carbonaceous material (organic carbon, OC) can comprise up to 90% of aerosol mass (Andreae and Crutzen, 1997; Cachier et al., 1995; Yamasoe et al., 2000), 10–70% of which may be water-soluble (WSOC). Studies have shown that WSOC can influence aerosol hygroscopicity and surface tension (Decesari et al., 2003; Saxena and Hildemann, 1996; Shulman et al., 1996) and must be characterized to quantify the impact of these aerosols on cloud droplet formation. WSOC can

Title Page

Abstract

Introduction

Conclusions

References

Tables

Figures

◀

▶

◀

▶

Back

Close

Full Screen / Esc

Printer-friendly Version

Interactive Discussion

be present in primary organic carbon but also formed during the oxidation of volatile organic carbon (VOC) to secondary organic aerosol (SOA) (Kanakidou et al., 2005; Robinson et al., 2007; Saxena and Hildemann, 1996).

Natural VOC emissions (e.g., monoterpenes, sesquiterpenes), estimated to be 1150 Tg yr⁻¹ (Guenther et al., 1995), are a major source of SOA. Alkene ozonolysis is well established as a source of SOA (e.g., Alfarra et al., 2006; Aschmann et al., 2002; Baltensperger et al., 2005; Claeys et al., 2004; Dommen et al., 2006; Shilling et al., 2007; Forstner et al., 1997; Gao et al., 2004a; Hamilton et al., 2006; Huff-Hartz et al., 2005; Kalberer et al., 2006; Kanakidou et al., 2005; Keywood et al., 2004; Kroll et al., 2006; Limbeck et al., 2003; Varutbangkul et al., 2006). Attempts to speciate SOA (Alfarra et al., 2006; Aschmann et al., 2002; Dommen et al., 2006; Gao et al., 2004a; Kalberer et al., 2006) have been met with limited success, as 80 to 90% of the aerosol mass can remain uncharacterized (Kalberer et al., 2006; Rogge et al., 1993; Seinfeld and Pandis, 1998). The potential for forming oligomeric or polymeric structures (Baltensperger et al., 2005; Gao et al., 2004a; Gao et al., 2004b; Kalberer et al., 2004) has been suggested to explain the uncharacterized SOA fraction. Oligomers have the potential to exhibit characteristics similar to humic-like substances (HULIS) (Baltensperger et al., 2005), which strongly depress surface tension (Asa-Awuku et al., 2007; Dinar et al., 2007; Graber and Rudich, 2006; Kiss et al., 2005; Salma et al., 2006) and potentially, droplet growth kinetics. All of these can have important impacts on CCN activity. Nevertheless, a complete thermodynamic characterization of the secondary aerosol, and of WSOC (required to constrain cloud droplet formation) have remained elusive (Kanakidou et al., 2005).

In this study we report the experimental investigation of the CCN activity of the water soluble fraction of SOA generated in laboratory chamber ozonolysis of alkenes; these measurements are then used to obtain thermodynamic properties (e.g., molar mass and surface tension depression), which are inferred using Köhler Theory Analysis (KTA) (Asa-Awuku et al., 2007; Padró et al., 2007). Furthermore, we characterize WSOC SOA droplet growth kinetics, relative to pure (NH₄)₂SO₄. Finally, we evaluate

**Köhler Theory
Analysis for SOA**

A. Asa-Awuku et al.

Title Page

Abstract

Introduction

Conclusions

References

Tables

Figures

◀

▶

◀

▶

Back

Close

Full Screen / Esc

Printer-friendly Version

Interactive Discussion

(by comparing inferred properties to direct measurements) the applications of KTA for complex organic aerosol systems.

2 Experimental methods and theoretical analysis

2.1 Filter extraction and chemical composition

5 Secondary organic aerosol is generated from the dark ozonolysis of three parent alkenes (cycloheptene, 1-methyl cycloheptene and terpinolene) and collected upon Teflon filters. The ozonolysis experiments were performed in the Caltech dual 28 m³ teflon chambers, a detailed description of which can be found in Keywood et al. (2004). SOA chemical speciation information measured by liquid chromatography/mass-spectrometry and ion trap mass spectrometry are available for the cycloheptene and 10 1-methylcycloheptene precursors from Gao et al. (2004a) (Table 1). No chemical speciation data are available for SOA generated from terpinolene. The presented analysis is the first study to characterize the CCN-relevant properties of WSOC from cycloheptene and 1-methyl cycloheptene ozonolysis. Table 1 presents the estimated average (mole fraction weighted) molar mass and carbon to organic carbon mass ratio for the 15 speciated organics.

Following the protocols outlined in Sullivan and Weber (2006), the WSOC in the filter samples was extracted in water during a 1.25 h sonication process with heat (water bath temperature ~60°C). WSOC concentration was then measured with a Total Organic Carbon (TOC) Turbo Siever analyzer (Sullivan and Weber, 2006). Anion concentrations (SO₄²⁻, Cl⁻ and NO₃⁻) of the extracted sample were measured with the Dionex 20 DX-500 ion chromatograph with Na₂CO₃/NaHCO₃ eluent and Metrosep A Supp 5-100 analytical column (Metrohm, Switzerland). Table 2 provides a summary of the offline WSOC chemical composition measurements and nominal anion concentrations in the 25 extracted samples; as expected, the ion concentrations are very low and contribute negligible solute to the samples. However, it is possible that the process of aerosol

Title Page

Abstract

Introduction

Conclusions

References

Tables

Figures

◀

▶

◀

▶

Back

Close

Full Screen / Esc

Printer-friendly Version

Interactive Discussion

collection, dissolution, atomization, and subsequent drying may affect the partitioning of CCN properties and growth kinetics of the SOA. In future studies, we will do both online and filter analysis to see whether the extraction process introduces significant artifacts.

5 2.2 CCN activity of SOA

The instruments and experimental set-up used to measure CCN activity are identical to those described in Asa-Awuku et al. (2007) and Padró et al. (2007). 3–5 ml of extracted sample is atomized in a collision type atomizer (University of Minnesota), dried with two diffusional driers and subsequently classified with a scanning mobility particle sizer (TSI SMPS 3080). The classified aerosol is then activated into droplets using a DMT Continuous Flow Thermal Gradient Chamber (Lance et al., 2006; Roberts and Nenes, 2005). The total concentration (CN) of sized particles is also counted, so that the ratio of CCN to CN can be determined. The process is repeated for different particle sizes. For each supersaturation, s , the cut-off diameter, d , (defined as the point at which CCN/CN=0.5) provides a quantitative characterization of the SOA CCN activity (i.e., for a given s , a larger d corresponds to a lower CCN activity).

2.3 Addition of inorganic salts

The impact of adding electrolytes to the CCN activity of the WSOC is explored by mixing a pre-calculated amount of $(\text{NH}_4)_2\text{SO}_4$ to the dissolved SOA sample (so that the salt mass fraction in the atomized aerosol is known). The mass of organic carbon, m_{organic} , in the extracted sample is determined by multiplying the measured WSOC carbon concentration by an organic carbon-to-carbon ratio of 2, as suggested by the speciated information provided by Gao et al. (2004a) (Table 1). The inorganic mass to be added, $m_{\text{inorganic}}$, to obtain the resulting inorganic mass fraction, α , is then computed

Title Page

Abstract

Introduction

Conclusions

References

Tables

Figures

◀

▶

◀

▶

Back

Close

Full Screen / Esc

Printer-friendly Version

Interactive Discussion

as,

$$m_{\text{inorganic}} = \frac{\alpha}{(1 - \alpha)} m_{\text{organic}} \quad (1)$$

where $m_{\text{organic}} = 2 \times [\text{WSOC}] V_{\text{sample}}$, $[\text{WSOC}]$ is the the WSOC concentration (mg C L^{-1}), and V_{sample} is the sample volume (ml). The 18 Mohms of filtered water used to extract the water during sonication contributes negligible ions to the particulate matter (Table 2).

2.4 Measuring and inferring surface tension of the CCN

A CAM 200 pendant drop method goniometer is used to directly measure surface tension. A description of the method and procedure can be found in Asa-Awuku et al. (2007). Since the surface tension depression strongly depends on $[\text{WSOC}]$ (Decesari et al., 2003; Henning et al., 2005; Kiss et al., 2005), surface tension, σ , is measured at numerous concentrations. The measurements are then fit to the Szyskowski-Langmuir isotherm (Asa-Awuku et al., 2007; Langmuir, 1917),

$$\sigma = \sigma_w - \alpha T \ln(1 + \beta c) \quad (2)$$

where σ_w is the surface tension of pure water at temperature, T , (obtained by infinitely diluting our sample with deionized ultra-filtered water), and α , β are empirical constants obtained from the fit. Unfortunately, direct measurement of σ of WSOC solutions at concentrations relevant for CCN activation (10^3 ppm and above) requires significant amount of mass ($10^3 \mu\text{g}$ and above) or usage of dilute WSOC sample. If α , β are based on using dilute samples, extrapolation of Eq. (2) to higher concentrations is often subject to substantial uncertainty because *i*) the uncertainty α and β can translate to large uncertainty in σ and *ii*) may not be applicable at concentrations close to or above the initial micelle concentration; we propose the following alternate method of inferring σ from CCN measurements.

As one approaches the critical micelle concentration for a solution containing organic surfactants and electrolytes, the surface tension of droplets would tend to vary little with

Title Page

Abstract

Introduction

Conclusions

References

Tables

Figures

◀

▶

◀

▶

Back

Close

Full Screen / Esc

Printer-friendly Version

Interactive Discussion

Köhler Theory Analysis for SOA

A. Asa-Awuku et al.

[Title Page](#)
[Abstract](#)
[Introduction](#)
[Conclusions](#)
[References](#)
[Tables](#)
[Figures](#)
[◀](#)
[▶](#)
[◀](#)
[▶](#)
[Back](#)
[Close](#)
[Full Screen / Esc](#)
[Printer-friendly Version](#)
[Interactive Discussion](#)

carbon concentration. Adding electrolytes can enhance surfactant partitioning to the surface layer (otherwise known as “salting-out” effect) (Asa-Awuku et al., 2007; Kiss et al., 2005). A ubiquitous bivalent ion, such as SO_4^{2-} can be a very effective “salting-out” agent, so that CCN containing surfactant and sulfate may have a constant surface tension (but lower than that of water). Salting-out and its effect on surface tension and CCN activity, has been seen in $(\text{NH}_4)_2\text{SO}_4$ – HULIS mixtures (Kiss et al., 2005) and hydrophobic water-soluble organics isolated from freshly collected biomass-burning aerosol (Asa-Awuku et al., 2007; Kiss et al., 2005).

Furthermore, if the salt mass fraction exceeds 50%, the majority of dissolved solute, n_s , is usually from the inorganic salt, and one could then infer the droplet surface tension, σ , at the point of activation using a combination of CCN activation experiments and Köhler theory, as follows. For particles composed of soluble and insoluble fractions, the critical supersaturation, s_c , is (Köhler, 1936; Seinfeld and Pandis, 1998),

$$s_c = \left(\frac{4A^3}{27B} \right)^{1/2} \quad (3)$$

where $A = \left(\frac{4M_w\sigma}{RT\rho_w} \right)$, $B = \left(\frac{6n_sM_w\nu}{\pi\rho_w} \right)$, R is the universal gas constant, T is droplet temperature, n_s are the moles of dissolved solute, with an effective Van’t Hoff factor ν . M_w and ρ_w are the molecular weight and density of water, respectively, and σ is the surface tension of the droplet at the point of activation. The assumption that the inorganic salt contributes the dominant solute implies it is the only component that contributes to B (otherwise known as the “Raoult term”),

$$B = \frac{M_w}{M_i} \frac{\rho_i}{\rho_w} d^3 \varepsilon_i \nu_i \quad (4)$$

where d is the CCN dry diameter, M_i is the molecular weight of the inorganic constituent, ε_i is the volume fraction of the inorganic which relates to mass fraction, m ,

and density, ρ , as

$$\varepsilon_i = \frac{m_i/\rho_i}{m_i/\rho_i + m_o/\rho_o} \quad (5)$$

where “i” and “o” subscripts refer to inorganic and organic components, respectively. If the organic is not a strong surfactant, then s_c for the dry diameter d and volume fraction ε_i , should be given by

$$s_c^* = \frac{2}{3} \left(\frac{4M_w\sigma_w}{RT\rho_w} \right)^{3/2} \left(3 \frac{M_w}{M_i} \frac{\rho_i}{\rho_w} d^3 \varepsilon_i \nu \right)^{-1/2} \quad (6)$$

where σ_w corresponds to the surface tension of pure water. However, if the organic depresses surface tension to σ (less than σ_w), then the critical supersaturation is given by

$$s_c = \frac{2}{3} \left(\frac{4M_w\sigma}{RT\rho_w} \right)^{3/2} \left(3 \frac{M_w}{M_i} \frac{\rho_i}{\rho_w} d^3 \varepsilon_i \nu \right)^{-1/2} \quad (7)$$

If s_c and d are known from the CCN activity measurements, Eqs. (6) and (7) can be combined to give σ :

$$\sigma = \sigma_w \left(\frac{s_c}{s_c^*} \right)^{2/3} \quad (8)$$

where s_c^* is given by Eq. (6); Eq. (8) represents the extension of Köhler Theory Analysis to infer surface tension from activation experiments. If the organic contribution to the Raoult term (Eq. 4) is not negligible, then it must be accounted for in Eqs. (6–8). Thus a molar volume must be calculated to estimate the organic contribution and the inferred surface tension is determined in conjunction with KTA (Sect. 2.5).

Title Page

Abstract

Introduction

Conclusions

References

Tables

Figures

◀

▶

◀

▶

Back

Close

Full Screen / Esc

Printer-friendly Version

Interactive Discussion

2.5 Köhler theory analysis (KTA) and molar volume uncertainty

KTA (Asa-Awuku et al., 2007; Padró et al., 2007) is used to infer average molar volume (molecular weight, M , over density ρ) of the water-soluble organic fraction of the SOA. KTA (method b_1 , Padró et al., 2007) employs measurements of dry diameter versus

- critical supersaturation, s_c , which are then fit to the expression, $s_c = \omega d^{-3}/2$. From the inferred CCN activity (INCA) parameter, ω , estimates of σ and measurements of ionic and WSOC concentrations, $\frac{M_o}{\rho_o}$ is obtained as,

$$\frac{M_o}{\rho_o} = \frac{\varepsilon_o v_o}{\frac{256}{27} \left(\frac{M_w}{\rho_w}\right)^2 \left(\frac{1}{RT}\right)^3 \sigma^3 \omega^{-2} - \frac{\rho_i}{M_i} \varepsilon_i v_i} \quad (9)$$

- KTA has been shown to constrain molecular weight estimates of known inorganic and organic mixtures to within 20% (Padró et al., 2007) and has also been applied to complex biomass burning WSOC with an estimated 40% uncertainty (Asa-Awuku et al., 2007).

- The measured variables employed in the KTA analysis are summarized in Table 3. In applying KTA, we assume that the effective organic Van't Hoff factor, $v_{\text{organic}}=1$. Molecular weights are presented assuming an average organic density of 1.4 g cm^{-3} (Turpin and Lim, 2001). The uncertainty in inferred molar volume can be computed as $\Delta \left(\frac{M_o}{\rho_o}\right) = \sqrt{\sum_{\text{for all } x} (\Phi_x \Delta x)^2}$, where Δx is the uncertainty in of each of the measured parameters x , (i.e., any of σ , ω , and v) and is the sensitivity of molar volume to x , $\Phi_x = \frac{\partial}{\partial x} \left(\frac{M_o}{\rho_o}\right)$, derived from Eq. (9). Table 4 provides a list of Φ_x .

2.6 Droplet growth kinetics

When exposed to the same s profile, an activated CCN will grow to cloud droplets of similar diameter, D_p , provided that the mass transfer coefficient of water vapor to the

Title Page

Abstract

Introduction

Conclusions

References

Tables

Figures

◀

▶

◀

▶

Back

Close

Full Screen / Esc

Printer-friendly Version

Interactive Discussion

growing droplet and the critical supersaturation is the same. The DMT CCN counter measures droplet sizes by an optical particle counter and therefore can be used to explore the impact of organics on the droplet growth kinetics. By comparing the droplet sizes of activated SOA particles against $(\text{NH}_4)_2\text{SO}_4$ particles at identical s_c , we directly assess the impact of organics on CCN growth kinetics. This is done by observing the wet diameter, D_p , that corresponds to particles with s_c equal to the instrument saturation, s , (i.e., CCN with a dry diameter equal to the cutoff diameter, d) and subsequently evaluating D_p versus s .

3 Results and discussion

3.1 CCN activity

The cut-off diameter, d , as a function of supersaturation and $(\text{NH}_4)_2\text{SO}_4$ mass fraction are shown for all SOA samples in Figs. 1–3. WSOC from the SOA for the three parent alkenes studied (Figs. 1, 2, and 3) indicate that as the mass fraction of $(\text{NH}_4)_2\text{SO}_4$ increases, the aerosol smoothly transitions to pure $(\text{NH}_4)_2\text{SO}_4$ behavior with roughly a $m_i^{-1/2}$ dependence. This suggests that the SOA are soluble hydrophilic relatively low molecular weight compounds that are not strong surfactants. For all three parent hydrocarbons, the original SOA samples activate at diameters larger than that of $(\text{NH}_4)_2\text{SO}_4$; this is expected as organics are, in general, less CCN active than $(\text{NH}_4)_2\text{SO}_4$. The activation curves are well represented with a power law consistent with a $d^{-3/2}$ dependence; this implies that the water-soluble SOA do not exhibit limited solubility (Padró et al., 2007).

3.2 Surface tension

Figure 4 shows the direct measurements of surface tension for all SOA samples and the Szyskowski-Langmuir fits to the data (α and β parameters of the fits are given in

Title Page

Abstract

Introduction

Conclusions

References

Tables

Figures

◀

▶

◀

▶

Back

Close

Full Screen / Esc

Printer-friendly Version

Interactive Discussion

**Köhler Theory
Analysis for SOA**

A. Asa-Awuku et al.

Title Page

Abstract

Introduction

Conclusions

References

Tables

Figures

◀

▶

◀

▶

Back

Close

Full Screen / Esc

Printer-friendly Version

Interactive Discussion

Table 2). None of the samples demonstrate significant surface tension depression at measured concentrations, even when extrapolated to concentrations relevant for CCN activation (100 mg C L^{-1} and above) (Fig. 4). If surfactants do exist in the SOA, it is likely they are not concentrated enough in the extracted samples to have a notable impact on surface tension; even for strong surfactants extracted from a biomass burning sample (Asa-Awuku et al., 2007), the depression for concentrations up to 100 mg C L^{-1} is within the measurement uncertainty (Fig. 4). Thus, direct surface tension measurements for dilute samples would not conclusively reveal the presence of surfactants. Acquiring sufficient sample for σ measurement is challenging, so we infer surface tension using the method described in Sect. 2.4. For large mass fractions of salt ($>90\%$), the inferred surface tension approaches that of water used to extract the WSOC from the SOA filter samples ($\sim 71 \text{ mN m}^{-1}$) (Table 5). However, for the 33% mixture of sulfate with cycloheptene and terpinolene, the inferred σ is $\sim 60 \text{ mN m}^{-1}$ (Table 5), $\sim 15\%$ depression from pure water, suggesting that surface active components do exist in the WSOC. The extent of surface tension depression suggests that the surfactants are appreciably strong, which is expected given the amphiphilic nature of the oxidation products; the presence of humic-like polymers (unless if in very small quantities) is unlikely, however given that expected depression is much higher at the point of activation (Asa-Awuku et al., 2007; Kiss et al., 2005; Salma et al., 2006).

3.3 Molecular weight estimates and uncertainty

Using the inferred values of surface tension (Table 5) and assuming an aerosol density of 1.4 g mol^{-1} (Turpin and Lim, 2001), KTA gives effective organic molecular weights of 162 ± 28 , 101 ± 20 , $207 \pm 54 \text{ g mol}^{-1}$ for terpinolene, 1-methylcycloheptene, and cycloheptene SOA, respectively (Tables 3 and 6), which are close to (that is within uncertainty of) the estimates from the Gao et al. (2004a) speciation (Table 1). If water surface tension was used to infer the molecular weight of the organics, large deviations from the Gao et al. (2004) speciations would be found (Tables 1 and 3) which includes low molecular weight diacids, carbonyl-containing acids, diacid alkeyl-

[Title Page](#)[Abstract](#)[Introduction](#)[Conclusions](#)[References](#)[Tables](#)[Figures](#)[◀](#)[▶](#)[◀](#)[▶](#)[Back](#)[Close](#)[Full Screen / Esc](#)[Printer-friendly Version](#)[Interactive Discussion](#)

sters, and hydroxyl diacids (e.g., pimelic acid, 160 g mol^{-1} ; adipic acid, 146 g mol^{-1} ; glutaric acid, 132 g mol^{-1} ; succinic acid, 118 g mol^{-1} ; pimelic acid monomethyl ester, 174 g mol^{-1} ; adipic acid monomethyl ester, 160 g mol^{-1} ; 2-hydroxypimelic acid, 176 g mol^{-1} ; 2-hydroxy glutaric acid, 148 g mol^{-1} ; 6-oxohexanoic acid, 130 g mol^{-1} and 6-oxo-7-hydroxyheptanoic acid, 158 g mol^{-1}). This correspondence validates the use of inferred σ values in KTA and to explore the presence of surfactants.

In terms of molar volume uncertainty, the assumption that $v_{\text{organic}} = 1$, does not account for the partial dissociation of the organic species. The greatest source of uncertainty in the calculations arise from v_{organic} (Table 6); v_{organic} larger than unity suggests larger molar volumes. The potential dissociation of organics (up to 20% as measured in HULIS titration experiments; Dinar et al., 2006), contributes roughly 23% uncertainty to the molar volume estimates. As in previous KTA studies (Asa-Awuku et al., 2007; Padró et al., 2007), the contributions of σ and ω variability to the inferred molar volume uncertainty are around 10% each. Uncertainty in molar mass (not molar volume) also arises from the value of density; varying from 1.4 g cm^{-3} to 1.6 g cm^{-3} (Turpin and Lim, 2001) increases molar masses by 14% (though relatively small compared to the uncertainty from v). The total estimated uncertainty in molar mass is approximately 25% for all SOA samples (Table 6).

3.4 Droplet growth kinetics

Figure 5 presents the droplet size measurements at the instrument OPC for all supersaturations and samples considered. For all points, the flow rate within the instrument was maintained constant at 0.5 L min^{-1} and the sheath to aerosol ratio is 10:1; this ensures that all the particles were exposed to similar supersaturation profiles. From Fig. 5 we conclude that the droplet growth kinetic curves for all SOA samples are virtually indistinguishable for all s values examined; compared to $(\text{NH}_4)_2\text{SO}_4$, SOA particles grow to very similar sizes. Only in some cases, does the organic CCN appear to grow slightly larger at higher supersaturations; this is attributed to water depletion effects from the

high concentrations of $(\text{NH}_4)_2\text{SO}_4$ particles within the instrument. Fewer particles of SOA ($\sim 600 \text{ cm}^{-3}$) do not deplete water vapor after activation, while whereas the higher concentration of $(\text{NH}_4)_2\text{SO}_4$ aerosols ($\sim 1800 \text{ cm}^{-3}$) after their activation deplete vapor faster than can be provided by diffusion. Although this does not affect CCN measurements, the supersaturation profile in the instrument changes slightly for the $(\text{NH}_4)_2\text{SO}_4$ calibration experiments, and D_p attained at the OPC is slightly decreased. Despite this, almost all of the growth kinetics experiments lie within the measurement uncertainty, so we conclude that the growth kinetics (or water vapor mass transfer coefficient) are uniform and equal to that of $(\text{NH}_4)_2\text{SO}_4$.

4 Summary and implications

In this study, we explore the CCN activity, composition, and droplet growth kinetic characteristics of SOA generated from the ozonolysis of biogenic precursors. A novel method is presented to infer surface tension depression from CCN activation experiments, which requires a much smaller aerosol sample than direct surface tension measurements at CCN-relevant concentrations. From the inferred values of surface tension we conclude that surfactants are likely present in the water-soluble fraction of the SOA, but with a smaller effect than expected for HULIS; together with the small average molar mass inferred from KTA (100 to 200 g mol^{-1}), this suggests that HULIS are not an important component of the WSOC fraction of the SOA studied here. KTA results are consistent with available composition data when using inferred surface tensions which validate the applicability of the method for complex mixtures. Finally we find that the presence of organic surfactants does not affect droplet growth kinetics; all the SOA samples exhibit growth kinetics similar to that of $(\text{NH}_4)_2\text{SO}_4$.

Acknowledgements. The work in this study is supported by a NSF CAREER Award and NASA Headquarters under the NASA Earth and Space Science Fellowship Program. Additional funding for the ozonolysis experiments and speciation was provided by the U.S. Department of Energy Biological and Environmental Research Program DE-FG00-05ER63983, Electric Power

Köhler Theory Analysis for SOA

A. Asa-Awuku et al.

[Title Page](#)[Abstract](#)[Introduction](#)[Conclusions](#)[References](#)[Tables](#)[Figures](#)[◀](#)[▶](#)[◀](#)[▶](#)[Back](#)[Close](#)[Full Screen / Esc](#)[Printer-friendly Version](#)[Interactive Discussion](#)

Research Institute, and U.S. Environmental Protection Agency RD-83107501-0. We would like to thank R. Weber and C. Hennigan of the Georgia Institute of Technology for the use of their Total Organic Carbon (TOC) Turbo Siever analyzer and Dionex DX-500 ion chromatograph.

References

- 5 Alfarra, M. R., Paulsen, D., Gysel, M., Garforth, A. A., Dommen, J., Prevot, A. S. H., Worsnop, D. R., Baltensperger, U., and Coe, H.: A mass spectrometric study of secondary organic aerosols formed from the photooxidation of anthropogenic and biogenic precursors in a reaction chamber, *Atmos. Chem. Phys.*, 6, 5279–5293, 2006, <http://www.atmos-chem-phys.net/6/5279/2006/>.
- 10 Andreae, M. O. and Crutzen, P. J.: Atmospheric aerosols: Biogeochemical sources and role in atmospheric chemistry, *Science*, 276, 1052–1058, 1997.
- Asa-Awuku, A., Nenes, A., Sullivan, A., Hennigan, C. J., and Weber, R. J.: Investigation of Molar Volume and Surfactant Characteristics of water-soluble Organic Compounds in Biomass Burning Aerosol, *Atmos. Chem. Phys. Discuss.*, 7, 3589–3627, 2007, <http://www.atmos-chem-phys-discuss.net/7/3589/2007/>.
- 15 Aschmann, S. M., Atkinson, R., and Arey, J.: Products of reaction of OH radicals with alpha-pinene, *J. Geophys. Res. Atmos.*, 107, 4191, doi:10.1029/2001JD001098, 2002.
- Baltensperger, U., Kalberer, M., Dommen, J., Paulsen, D., Alfarra, M. R., Coe, H., Fisseha, R., Gascho, A., Gysel, M., Nyeki, S., Sax, M., Steinbacher, M., Prevot, A. S. H., Sjoren, S., Weingartner, E., and Zenobi, R.: Secondary organic aerosols from anthropogenic and biogenic precursors, *Faraday Discuss.*, 130, 265–278, 2005.
- 20 Cachier, H., Lioussé, C., Buatmenard, P., and Gaudichet, A.: Particulate Content Of Savanna Fire Emissions, *J. Atmos. Chem.*, 22, 123–148, 1995.
- Claeys, M., Wang, W., Ion, A. C., Kourtchev, I., Gelencser, A., and Maenhaut, W.: Formation of secondary organic aerosols from isoprene and its gas-phase oxidation products through reaction with hydrogen peroxide, *Atmos. Environ.*, 38, 4093–4098, 2004.
- 25 Decesari, S., Facchini, M. C., Mircea, M., Cavalli, F., and Fuzzi, S.: Solubility properties of surfactants in atmospheric aerosol and cloud/fog water samples, *J. Geophys. Res. Atmos.*, 108, 4685, doi:10.1029/2003JD003566, 2003.
- 30 Dinar, E., Taraniuk, I., Graber, E. R., Anttila, T., Mentel, T. F., and Rudich, Y.: Hygroscopic

Köhler Theory Analysis for SOA

A. Asa-Awuku et al.

Title Page

Abstract

Introduction

Conclusions

References

Tables

Figures

◀

▶

◀

▶

Back

Close

Full Screen / Esc

Printer-friendly Version

Interactive Discussion

**Köhler Theory
Analysis for SOA**

A. Asa-Awuku et al.

Title Page

Abstract

Introduction

Conclusions

References

Tables

Figures

◀

▶

◀

▶

Back

Close

Full Screen / Esc

Printer-friendly Version

Interactive Discussion

growth of atmospheric and model humic-like substances, *J. Geophys. Res. Atmos.*, 112, D05211, doi:10.1029/2006JD007442 2007.

Dinar, E., Taraniuk, I., Graber, E. R., Katsman, S., Moise, T., Anttila, T., Mentel, T. F., and Rudich, Y.: Cloud Condensation Nuclei properties of model and atmospheric HULIS, *Atmos. Chem. Phys.*, 6, 2465–2481, 2006,
5 <http://www.atmos-chem-phys.net/6/2465/2006/>.

Dommen, J., Metzger, A., Duplissy, J., Kalberer, M., Alfarra, M. R., Gascho, A., Weingartner, E., Prevot, A. S. H., Verheggen, B., and Baltensperger, U.: Laboratory observation of oligomers in the aerosol from isoprene/NO_x photooxidation, *Geophys. Res. Lett.*, 33, L13805, doi:10.1029/2006GL026523, 2006.

Forstner, H. J. L., Flagan, R. C., and Seinfeld, J. H.: Secondary organic aerosol from the photooxidation of aromatic hydrocarbons: Molecular composition, *Environ. Sci. Tech.*, 31, 1345–1358, 1997.

Gao, S., Keywood, M., Ng, N. L., Surratt, J., Varutbangkul, V., Bahreini, R., Flagan, R. C., and Seinfeld, J. H.: Low-molecular-weight and oligomeric components in secondary organic aerosol from the ozonolysis of cycloalkenes and alpha-pinene, *J. Phys. Chem. A*, 10 147–10 164, 2004a.

Gao, S., Ng, N. L., Keywood, M., Varutbangkul, V., Bahreini, R., Nenes, A., He, J. W., Yoo, K. Y., Beauchamp, J. L., Hodyss, R. P., Flagan, R. C., and Seinfeld, J. H.: Particle phase acidity and oligomer formation in secondary organic aerosol, *Environ. Sci. Tech.*, 38, 6582–6589, 2004b.

Graber, E. R. and Rudich, Y.: Atmospheric HULIS: How humic-like are they? A comprehensive and critical review, *Atmos. Chem. Phys.*, 6, 729–753, 2006,
15 <http://www.atmos-chem-phys.net/6/729/2006/>.

Guenther, A., Hewitt, C. N., Erickson, D., Fall, R., Geron, C., Graedel, T., Harley, P., Klinger, L., Lerdau, M., McKay, W. A., Pierce, T., Scholes, B., Steinbrecher, R., Tallamraju, R., Taylor, J., and Zimmerman, P.: A Global-Model of Natural Volatile Organic-Compound Emissions, *J. Geophys. Res. Atmos.*, 100, 8873–8892, 1995.

Hamilton, J. F., Lewis, A. C., Reynolds, J. C., Carpenter, L. J., and Lubben, A.: Investigating the composition of organic aerosol resulting from cyclohexene ozonolysis: low molecular weight and heterogeneous reaction products, *Atmos. Chem. Phys.*, 6, 4973–4984, 2006,
20 <http://www.atmos-chem-phys.net/6/4973/2006/>.

Henning, S., Rosenorn, T., D’Anna, B., Gola, A. A., Svenningsson, B., and Bilde, M.: Cloud

droplet activation and surface tension of mixtures of slightly soluble organics and inorganic salt, *Atmos. Chem. Phys.*, 5, 575–582, 2005,

<http://www.atmos-chem-phys.net/5/575/2005/>.

5 Huff-Hartz, K. E., Rosenorn, T., Ferchak, S. R., Raymond, T. M., Bilde, M., Donahue, N. M., and Pandis, S. N.: Cloud condensation nuclei activation of monoterpene and sesquiterpene secondary organic aerosol, *J. Geophys. Res. Atmos.*, 110, D14208, doi:10.1029/2004JD005754, 2005.

10 Kalberer, M., Paulsen, D., Sax, M., Steinbacher, M., Dommen, J., Prevot, A. S. H., Fisseha, R., Weingartner, E., Frankevich, V., Zenobi, R., and Baltensperger, U.: Identification of polymers as major components of atmospheric organic aerosols, *Science*, 303, 1659–1662, 2004.

Kalberer, M., Sax, M., and Samburova, V.: Molecular size evolution of oligomers in organic aerosols collected in urban atmospheres and generated in a smog chamber, *Environ. Sci. Tech.*, 40, 5917–5922, 2006.

15 Kanakidou, M., Seinfeld, J. H., Pandis, S. N., Barnes, I., Dentener, F. J., Facchini, M. C., Van Dingenen, R., Ervens, B., Nenes, A., Nielsen, C. J., Swietlicki, E., Putaud, J. P., Balkanski, Y., Fuzzi, S., Horth, J., Moortgat, G. K., Winterhalter, R., Myhre, C. E. L., Tsigaridis, K., Vignati, E., Stephanou, E. G., and Wilson, J.: Organic aerosol and global climate modelling: a review, *Atmos. Chem. Phys.*, 5, 1053–1123, 2005,

<http://www.atmos-chem-phys.net/5/1053/2005/>.

20 Keyword, M. D., Varutbangkul, V., Bahreini, R., Flagan, R. C., and Seinfeld, J. H.: Secondary organic aerosol formation from the ozonolysis of cycloalkenes and related compounds, *Environ. Sci. Tech.*, 38, 4157–4164, 2004.

Kiss, G., Tombacz, E., and Hansson, H. C.: Surface tension effects of humic-like substances in the aqueous extract of tropospheric fine aerosol, *J. Atmos. Chem.*, 50, 279–294, 2005.

25 Köhler, H.: The nucleus in and the growth of hygroscopic droplets, *Transactions of the Faraday Society*, 43, 1152–1161, 1936.

Kroll, J. H., Ng, N. L., Murphy, S. M., Flagan, R. C., and Seinfeld, J. H.: Secondary organic aerosol formation from isoprene photooxidation, *Environ. Sci. Tech.*, 40, 1869–1877, 2006.

Lance, S., Medina, J., Smith, J. N., and Nenes, A.: Mapping the operation of the DMT Continuous Flow CCN counter, *Aerosol Sci. Tech.*, 40, 242–254, 2006.

30 Langmuir, I.: The constitution and fundamental properties of solids and liquids. II. Liquids, *J. Am. Chem. Soc.*, 39, 1848–1906, 1917.

Limbeck, A., Kulmala, M., and Puxbaum, H.: Secondary organic aerosol formation in the atmo-

**Köhler Theory
Analysis for SOA**

A. Asa-Awuku et al.

Title Page

Abstract

Introduction

Conclusions

References

Tables

Figures

◀

▶

◀

▶

Back

Close

Full Screen / Esc

Printer-friendly Version

Interactive Discussion

- sphere via heterogeneous reaction of gaseous isoprene on acidic particles, *Geophys. Res. Lett.*, 30, 1996, doi:10.1029/2003GL017738, 2003.
- Padró, L. T., Asa-Awuku, A., Morisson, R., and Nenes, A.: Inferring Thermodynamic Properties from CCN Activation Experiments a) Single-component and Binary Aerosols, *Atmos. Chem. Phys. Discuss.*, 7, 3805–3836, 2007,
5 <http://www.atmos-chem-phys-discuss.net/7/3805/2007/>.
- Roberts, G. C., and Nenes, A.: A continuous-flow streamwise thermal-gradient CCN chamber for atmospheric measurements, *Aerosol Sci. Tech.*, 39, 206–221, 2005.
- Robinson, A. L., Donahue, N. M., Shrivastava, M. K., Weitkamp, E. A., Sage, A. M., Grieshop, A. P., Lane, T. E., Pierce, J. R., and Pandis, S. N.: Rethinking organic aerosols: Semivolatile emissions and photochemical aging, *Science*, 315, 1259–1262, 2007.
- 10 Rogge, W. F., Mazurek, M. A., Hildemann, L. M., Cass, G. R., and Simoneit, B. R. T.: Quantification of Urban Organic Aerosols at a Molecular-Level – Identification, Abundance and Seasonal-Variation, *Atmospheric Environment Part a-General Topics*, 27, 1309–1330, 1993.
- 15 Salma, I., Ocskay, R., Varga, I., and Maenhaut, W.: Surface tension of atmospheric humic-like substances in connection with relaxation, dilution, and solution pH, *J. Geophys. Res. Atmos.*, 111, D23205, doi:10.1029/2005JD007015, 2006.
- Saxena, P., and Hildemann, L. M.: Water-soluble organics in atmospheric particles: A critical review of the literature and application of thermodynamics to identify candidate compounds, *J. Atmos. Chem.*, 24, 57–109, 1996.
- 20 Seinfeld, J. H., and Pandis, S. N.: *Atmospheric Chemistry & Physics: From Air Pollution to Climate Change*, John Wiley & Sons, 1998.
- Shilling, J. E., King, S. M., Mochida, M., and Martin, S. T.: Mass spectral evidence that small changes in composition caused by oxidative aging processes alter aerosol CCN properties, *J. Phys. Chem.*, 111, 3358–3368, 2007.
- 25 Shulman, M. L., Jacobson, M. C., Carlson, R. J., Synovec, R. E., and Young, T. E.: Dissolution behavior and surface tension effects of organic compounds in nucleating cloud droplets, *Geophys. Res. Lett.*, 23, 277–280, 1996.
- Sullivan, A. P. and Weber, R. J.: Chemical characterization of the ambient organic aerosol soluble in water: 1. Isolation of hydrophobic and hydrophilic fractions with a XAD-8 resin, *J. Geophys. Res. Atmos.*, 111, D05314, doi:10.1029/2005JD006485, 2006.
- 30 Turpin, B. J. and Lim, H. J.: Species contributions to PM_{2.5} mass concentrations: Revisiting common assumptions for estimating organic mass, *Aerosol Sci. Tech.*, 35, 602–610, 2001.

**Köhler Theory
Analysis for SOA**

A. Asa-Awuku et al.

Title Page

Abstract

Introduction

Conclusions

References

Tables

Figures

◀

▶

◀

▶

Back

Close

Full Screen / Esc

Printer-friendly Version

Interactive Discussion

Varutbangkul, V., Brechtel, F. J., Bahreini, R., Ng, N. L., Keywood, M. D., Kroll, J. H., Flagan, R. C., Seinfeld, J. H., Lee, A., and Goldstein, A. H.: Hygroscopicity of secondary organic aerosols formed by oxidation of cycloalkenes, monoterpenes, sesquiterpenes, and related compounds, *Atmos. Chem. Phys.*, 6, 2367–2388, 2006,

5 <http://www.atmos-chem-phys.net/6/2367/2006/>.

Yamasoe, M. A., Artaxo, P., Miguel, A. H., and Allen, A. G.: Chemical composition of aerosol particles from direct emissions of vegetation fires in the Amazon Basin: water-soluble species and trace elements, *Atmos. Environ.*, 34, 1641-1-653, 2000.

ACPD

7, 8983–9011, 2007

Köhler Theory Analysis for SOA

A. Asa-Awuku et al.

Title Page

Abstract

Introduction

Conclusions

References

Tables

Figures

◀

▶

◀

▶

Back

Close

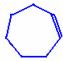

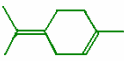
Full Screen / Esc

Printer-friendly Version

Interactive Discussion

EGU

Table 1. Characteristics of parent hydrocarbons and water-soluble fraction of SOA.

Hydrocarbon precursor	Cycloheptene	1-methylcycloheptene	Terpinolene
Structure			
O ₃ concentration (ppb) for forming SOA	200	171	188
Major Type of Compounds Identified	Low Molecular Weight Compounds (<250 g mol ⁻¹)	Low Molecular Weight Compounds (<250 g mol ⁻¹) ^a	Not Available
Classes speciated	diacids, carbonyl-containing acids, diacid alkyl esters and hydroxy diacids	diacids, carbonyl-containing acids, diacid alkyl esters and hydroxy diacids ^a	Not Available
Major slightly soluble organic components identified (< 0.1 g/100 g H ₂ O)	2 Hydroxy Pimelic Acid [176 g mol ⁻¹] Pimelic Acid [160 g mol ⁻¹] Adipic Acid [146 g mol ⁻¹]	Adipic Acid ^a [146 g mol ⁻¹] Pimelic Acid ^a [160 g mol ⁻¹] Adipic Acid Monomethyl Ester ^a [160 g mol ⁻¹]	Not Available
Major soluble organic component (> 0.1 g/100 g H ₂ O)	Glutaric Acid [132 g mol ⁻¹]	6,7-dioxoheptanoic Acid ^a [158 g mol ⁻¹] Glutaric Acid ^a [132 g mol ⁻¹]	Not Available
% Low Molecular weight species from total SOA mass derived from DMA measurements	34	44 ^a	Not Available
Number Averaged molecular weight of the speciated components	150	147 ^a	Not Available
Average mass ratio of carbon to organic carbon from speciated components	0.50	0.50 ^a	Not Available

Obtained from Gao et al. (2004a)

^a Information obtained from 1-methylcyclohexene ozonolysis due to its structural similarity.

Title Page

Abstract

Introduction

Conclusions

References

Tables

Figures

◀

▶

◀

▶

Back

Close

Full Screen / Esc

Printer-friendly Version

Interactive Discussion

Köhler Theory Analysis for SOA

A. Asa-Awuku et al.

Table 2. Summary of WSOC and ion concentrations, α and β parameters of the Szyszkowski-Langmuir isotherm for all SOA considered. Measured Cl^- , SO_4^{2-} and NO_3^- concentrations were all below $2.55 \times 10^{-5} \text{ mg L}^{-1}$.

Parent Hydrocarbon	WSOC (mg C L^{-1})	α ($\text{mN m}^{-1} \text{K}^{-1}$)	β^b (L mg^{-1})
Cycloheptene	13	2.59	1×10^{-6}
1-methylcycloheptene	6	4.82×10^{-5}	4.63×10^{-19}
Terpinolene	10	92.5	1×10^{-13}

^b Measurements are taken at room temperature between 296 and 299 K.

[Title Page](#)
[Abstract](#)
[Introduction](#)
[Conclusions](#)
[References](#)
[Tables](#)
[Figures](#)
[Back](#)
[Close](#)
[Full Screen / Esc](#)
[Printer-friendly Version](#)
[Interactive Discussion](#)

Köhler Theory Analysis for SOA

A. Asa-Awuku et al.

Table 3. Köhler Theory Analysis Properties and Molar Volume Results.

Property (units)	Cycloheptene	1-methylcycloheptene	Terpinolene
ω (m ^{1.5})	7.14×10^{-14}	5.67×10^{-14}	6.53×10^{-14}
σ (N m ⁻¹) ^c	5.99×10^{-2}	6.52×10^{-2}	6.11×10^{-2}
$\left(\frac{M_o}{\rho_o}\right)$ (m ³ mol ⁻¹)	1.44×10^{-4}	5.69×10^{-5}	7.54×10^{-5}
M_o (g mol ⁻¹) ^d	207 ^c (126) ^e	101 ^c (80) ^e	162 ^c (106) ^e

^c Inferred from activation experiments (Table 5).

^d Assuming the density of the solute is assumed to be 1400 kg m⁻³ (Turpin and Lim, 2001).

^e KTA Results based on $\sigma = \sigma_{\text{water}}$ (72 mN m⁻¹).

[Title Page](#)
[Abstract](#)
[Introduction](#)
[Conclusions](#)
[References](#)
[Tables](#)
[Figures](#)
[Back](#)
[Close](#)
[Full Screen / Esc](#)
[Printer-friendly Version](#)
[Interactive Discussion](#)

Table 4. Formulae for the Sensitivity of Molar Volume to the dependant parameters σ , ω , and V_o .

Property	Sensitivity, $\Phi_x = \frac{\partial}{\partial x} \left(\frac{M_o}{\rho_o} \right)$
σ	$\Phi_\sigma = \left(\frac{3 \times 256}{27} \left(\frac{M_w}{\rho_w} \right)^2 \left(\frac{1}{RT} \right)^3 \frac{\sigma^2 \omega^{-2}}{\varepsilon_o V_o} \right) \left(\frac{M_o}{\rho_o} \right)^2$
ω	$\Phi_\omega = \left(\frac{2 \times 256}{27} \left(\frac{M_w}{\rho_w} \right)^2 \left(\frac{1}{RT} \right)^3 \frac{\sigma^3 \omega^{-3}}{\varepsilon_o V_o} \right) \left(\frac{M_o}{\rho_o} \right)^2$
V_o	$\Phi_{V_o} = \frac{256}{27} \left(\frac{M_w}{\rho_w} \right)^2 \left(\frac{1}{RT} \right)^3 \frac{-\sigma^3 \omega^{-2} V_o^{-2}}{\varepsilon_o} \left(\frac{M_o}{\rho_o} \right)^2 + \left(\sum_{i \neq j} \frac{\rho_i \varepsilon_i V_i}{M_i \varepsilon_o} \right) V_o^{-2} \left(\frac{M_o}{\rho_o} \right)^2$

[Title Page](#)
[Abstract](#)
[Introduction](#)
[Conclusions](#)
[References](#)
[Tables](#)
[Figures](#)
[◀](#)
[▶](#)
[◀](#)
[▶](#)
[Back](#)
[Close](#)
[Full Screen / Esc](#)
[Printer-friendly Version](#)
[Interactive Discussion](#)

Köhler Theory Analysis for SOA

A. Asa-Awuku et al.

Table 5. σ values inferred at the point of activation.

Sample	σ (mN m^{-1})	$\pm \Delta\sigma$ (mN m^{-1})
Cycloheptene SOA with 90% $(\text{NH}_4)_2\text{SO}_4$	73.6	4.6
Cycloheptene SOA with 33% $(\text{NH}_4)_2\text{SO}_4$	59.9	1.9
1-methylcycloheptene SOA with 33 % $(\text{NH}_4)_2\text{SO}_4$	65.2	2.5
Terpinolene SOA with 98% $(\text{NH}_4)_2\text{SO}_4$	74.4	4.9
Terpinolene SOA with 90% $(\text{NH}_4)_2\text{SO}_4$	70.5	4.0
Terpinolene SOA with 33% $(\text{NH}_4)_2\text{SO}_4$	61.1	7.9

Title Page

Abstract

Introduction

Conclusions

References

Tables

Figures

◀

▶

◀

▶

Back

Close

Full Screen / Esc

Printer-friendly Version

Interactive Discussion

Table 6. Molar Volume Sensitivity Analysis for SOA.

SOA Precursor Hydrocarbon	Property x (units)	Δx	Φ_x ($\text{m}^3 \text{mol}^{-1} \text{x}^{-1}$)	Molar volume uncertainty (%)
Terpinolene	σ	1.41×10^{-3}	3.73×10^{-3}	7.0
	ω	2.21×10^{-15}	2.69×10^9	7.9
	v_{organic}	0.20^{f}	8.78×10^{-5}	23.3
	<i>Total Uncertainty</i>			26.2
	1-methylcycloheptene	σ	1.40×10^{-3}	2.76×10^{-3}
ω		1.90×10^{-15}	2.26×10^9	7.5
v_{organic}		0.20^{f}	6.41×10^{-5}	22.5
<i>Total Uncertainty</i>				25.1
Cycloheptene		σ	1.21×10^{-3}	8.34×10^{-3}
	ω	1.58×10^{-15}	4.71×10^9	5.2
	v_{organic}	0.20^{f}	1.68×10^{-4}	23.3
	<i>Total Uncertainty</i>			26.9

^f Error based on observations of 20% disassociation of organic HULIS in titration experiments Dinar et al. (2006).

[Title Page](#)
[Abstract](#)
[Introduction](#)
[Conclusions](#)
[References](#)
[Tables](#)
[Figures](#)
[◀](#)
[▶](#)
[◀](#)
[▶](#)
[Back](#)
[Close](#)
[Full Screen / Esc](#)
[Printer-friendly Version](#)
[Interactive Discussion](#)

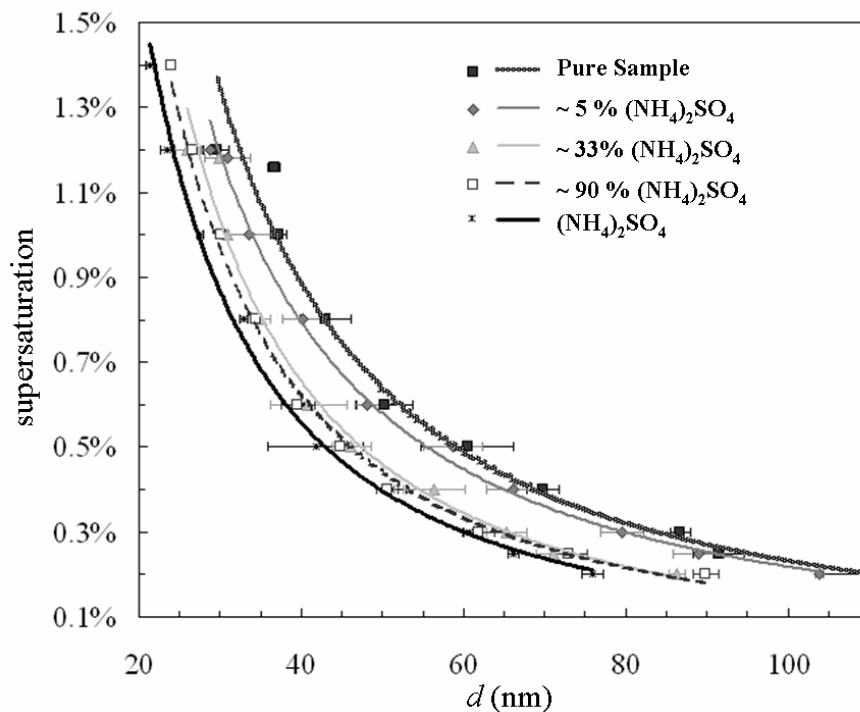


Fig. 1. CCN activity of WSOC generated from ozonolysis of cycloheptene. Results are shown for pure WSOC and mixtures of $(\text{NH}_4)_2\text{SO}_4$. The cut-off diameter, d , is the point at which $\text{CCN}/\text{CN}=0.5$ is plotted versus supersaturation.

[Title Page](#)[Abstract](#)[Introduction](#)[Conclusions](#)[References](#)[Tables](#)[Figures](#)[◀](#)[▶](#)[◀](#)[▶](#)[Back](#)[Close](#)[Full Screen / Esc](#)[Printer-friendly Version](#)[Interactive Discussion](#)

EGU

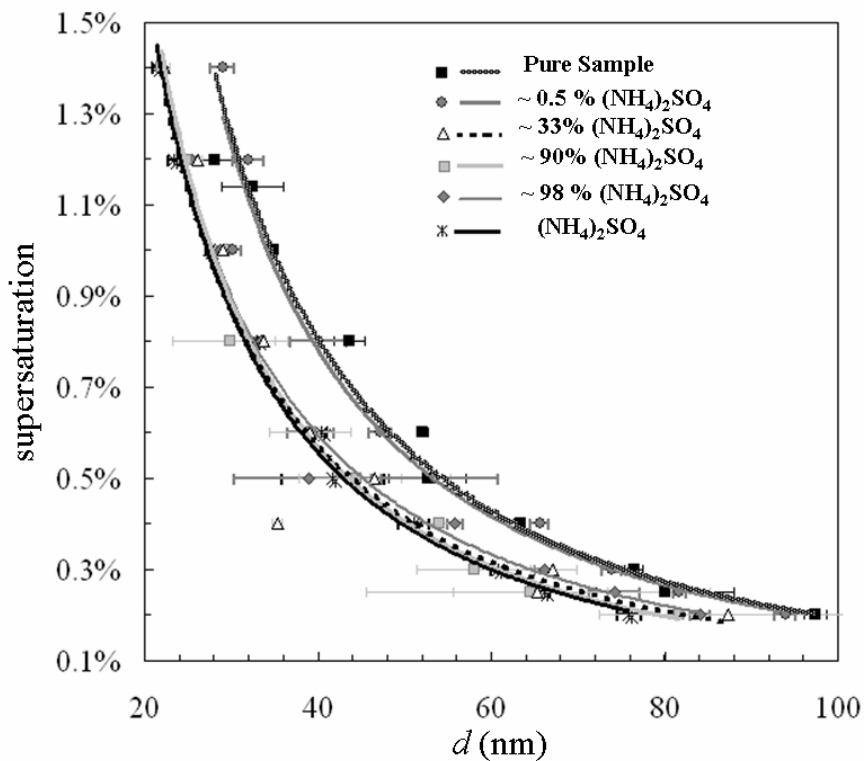


Fig. 2. CCN activity of WSOC generated from ozonolysis of terpinolene. Results are shown for pure WSOC and mixtures of $(\text{NH}_4)_2\text{SO}_4$. The cut-off diameter, d , is the point at which $\text{CCN}/\text{CN}=0.5$ is plotted versus supersaturation.

[Title Page](#)
[Abstract](#)
[Introduction](#)
[Conclusions](#)
[References](#)
[Tables](#)
[Figures](#)
[◀](#)
[▶](#)
[◀](#)
[▶](#)
[Back](#)
[Close](#)
[Full Screen / Esc](#)
[Printer-friendly Version](#)
[Interactive Discussion](#)

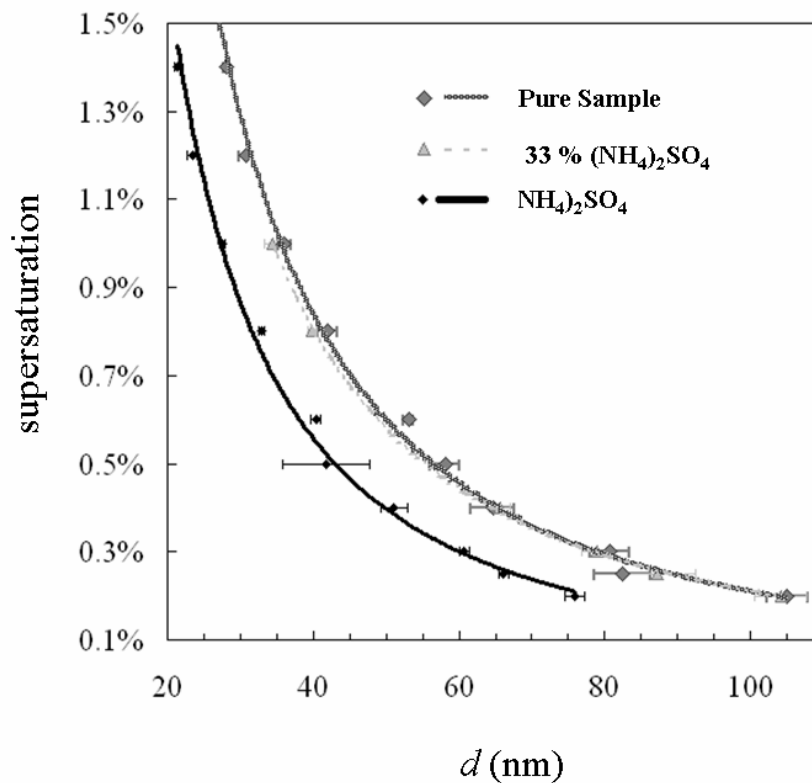


Fig. 3. CCN activity of WSOC generated from ozonolysis of 1-methylcycloheptene. Results are shown for pure WSOC and mixtures of $(\text{NH}_4)_2\text{SO}_4$. The cut-off diameter, d , is the point at which $\text{CCN}/\text{CN}=0.5$ is plotted versus supersaturation.

[Title Page](#)[Abstract](#)[Introduction](#)[Conclusions](#)[References](#)[Tables](#)[Figures](#)[◀](#)[▶](#)[◀](#)[▶](#)[Back](#)[Close](#)[Full Screen / Esc](#)[Printer-friendly Version](#)[Interactive Discussion](#)

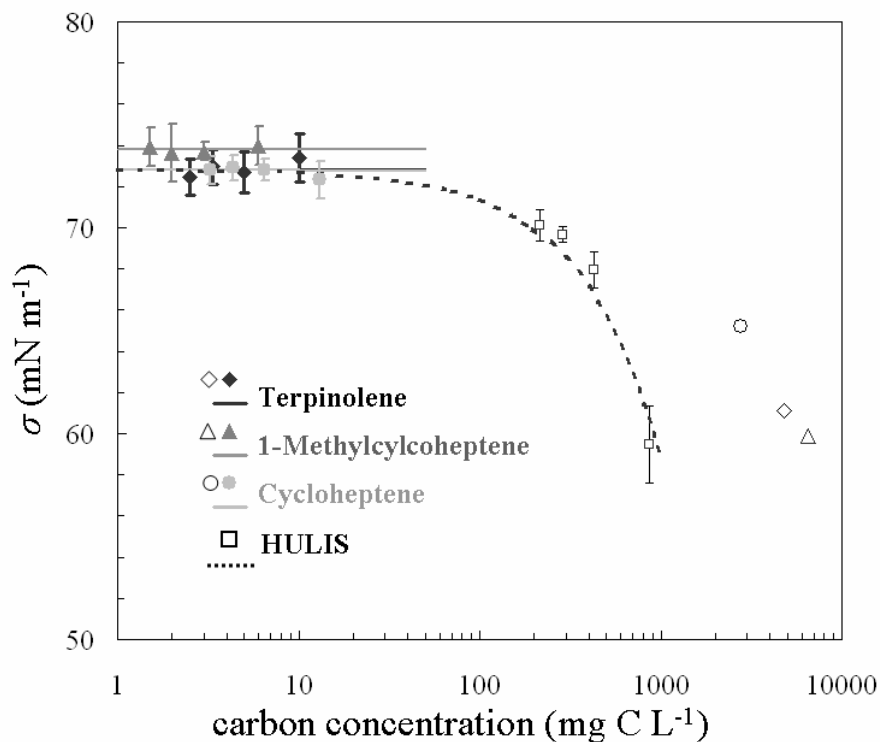


Fig. 4. Direct σ measurements of SOA as a function of water-soluble carbon concentration (closed symbols) and inferred values from (Table 5) (open SOA symbols) as a function of water soluble carbon concentration at activation. Curves represent Szyskowski-Langmuir isotherm fits of experimental data. HULIS data from Asa-Awuku et al. (2007) is provided for comparison.

[Title Page](#)[Abstract](#)[Introduction](#)[Conclusions](#)[References](#)[Tables](#)[Figures](#)[◀](#)[▶](#)[◀](#)[▶](#)[Back](#)[Close](#)[Full Screen / Esc](#)[Printer-friendly Version](#)[Interactive Discussion](#)

EGU

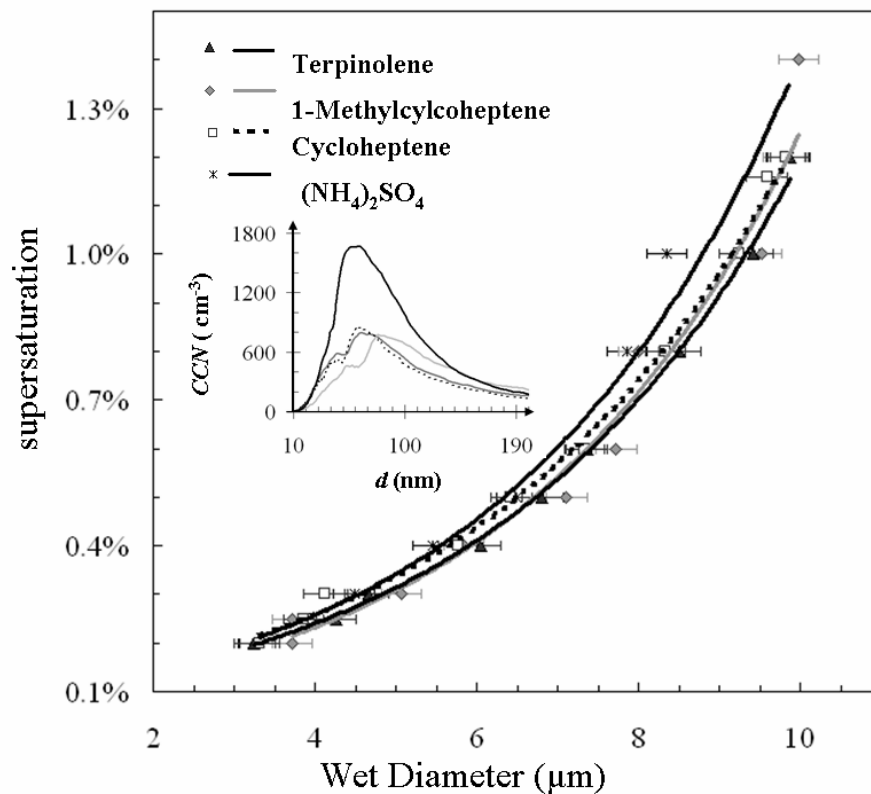


Fig. 5. Growth kinetic measurements for SOA and $(\text{NH}_4)_2\text{SO}_4$ CCN. Inset graph corresponds to the CCN concentration-dry diameter histogram determined at a 10:1 sheath to aerosol ratio as a function of mean dry diameter at 1% supersaturation.

[Title Page](#)[Abstract](#)[Introduction](#)[Conclusions](#)[References](#)[Tables](#)[Figures](#)[◀](#)[▶](#)[◀](#)[▶](#)[Back](#)[Close](#)[Full Screen / Esc](#)[Printer-friendly Version](#)[Interactive Discussion](#)

EGU